Journal of Molecular Structure 1048 (2013) 420–425

Contents lists available at SciVerse ScienceDirect

Journal of Molecular Structure

journal homepage: www.elsevier.com/locate/molstruc

The molecular structure of the phosphate mineral senegalite $Al_2(PO_4)(OH)_3{\cdot}3H_2O$ – A vibrational spectroscopic study

Ray L. Frost [a,*], Andrés López [a], Yunfei Xi [a], Natália Murta [b], Ricardo Scholz [c]

[a] School of Chemistry, Physics and Mechanical Engineering, Science and Engineering Faculty, Queensland University of Technology, GPO Box 2434, Brisbane, Queensland 4001, Australia
[b] Mining Engineering Department, School of Mines, Federal University of Ouro Preto, Campus Morro do Cruzeiro, Ouro Preto, MG 35,400-00, Brazil
[c] Geology Department, School of Mines, Federal University of Ouro Preto, Campus Morro do Cruzeiro, Ouro Preto, MG 35,400-00, Brazil

HIGHLIGHTS

- We have studied the mineral senagalite, a hydrated hydroxy phosphate of aluminium with formula $Al_2(PO_4)(OH)_3{\cdot}3H_2O$.
- A combination of electron microscopy and vibrational spectroscopy was used.
- Senegalite crystal aggregates shows tabular to prismatic habitus and orthorhombic form.
- A comparison is made with spectra of other aluminium containing phosphate minerals such as augelite and turquoise.
- Vibrational spectroscopy offers a means for the assessment of the structure of senagalite.

ARTICLE INFO

Article history:
Received 10 April 2013
Accepted 27 May 2013
Available online 1 June 2013

Keywords:
Senegalite
Phosphate
Pegmatite
Raman spectroscopy
Infrared spectroscopy

ABSTRACT

We have studied the mineral senagalite, a hydrated hydroxy phosphate of aluminium with formula $Al_2(PO_4)(OH)_3{\cdot}3H_2O$ using a combination of electron microscopy and vibrational spectroscopy. Senegalite crystal aggregates shows tabular to prismatic habitus and orthorhombic form. The Raman spectrum is dominated by an intense band at 1029 cm^{-1} assigned to the PO_4^{3-} ν_1 symmetric stretching mode. Intense Raman bands are found at 1071 and 1154 cm^{-1} with bands of lesser intensity at 1110, 1179 and 1206 cm^{-1} and are attributed to the PO_4^{3-} ν_3 antisymmetric stretching vibrations. The infrared spectrum shows complexity with a series overlapping bands. A comparison is made with spectra of other aluminium containing phosphate minerals such as augelite and turquoise. Multiple bands are observed for the phosphate bending modes giving support for the reduction of symmetry of the phosphate anion. Vibrational spectroscopy offers a means for the assessment of the structure of senagalite.

1. Introduction

Senegalite is a hydrated hydroxy phosphate of aluminium of formula $Al_2(PO_4)(OH)_3{\cdot}3H_2O$ [1]. The mineral originated from Kouroudiako iron deposit, Faleme river basin, Senegal. The mineral is orthorhombic [2,3] with point group *mm*2 with *a* 7.675(4), *b* 9.711(4), and *c* 7.635(4) Å, *Z* = 4. According to Keegan et al. [2] the mineral possesses a new structure type based on chains. According to Keegan et al. [2] two symmetry-equivalent chains run parallel to [1 0 1] and [1 0 1], each based on distorted $Al(OH)_3(H_2O)(Op)_2$ (Op = phosphate oxygen) octahedral and $Al(OH)_3(Op)_2$ trigonal bipyramid edge-sharing dimers which further corner-link to complete the chain. Corner-linking (PO_4) tetrahedra knit neighbouring chains to form an open sheet parallel to (0 1 0). The mineral shows yellowish-green prismatic crystals.

The phosphates of copper are many and varied but of the other divalent cations such as zinc, the phosphates are quite rare. In contrast the phosphates of the trivalent cations such as Al^{3+} and Fe^{3+} are many and varied. There can be much isomorphic substitution. The structure of augelite was first determined by Araki et al. [4]. The building blocks in augelite are tetranuclear entities formed by symmetry correlated pairs of condensed octahedra AlO_6 and trigonal bipyramids AlO_5 which are linked by phosphate groups [4]. This paper does not mention hydrogen bonds but from the data given two independent O–H···O distances can be estimated. More recent work gave two O–D···O distances for synthetic augelite-d3 [5]. Huminicki and Hawthorne discuss the crystal chemistry of the phosphate minerals and list some 121 different phosphate minerals of these two elements [6]. Great variation in the structure of the phosphate minerals occurs [6]. The primary fundamental characteristic of a mineral is its crystal structure which defines the identities, amounts and arrangements of atoms that comprise the crystal. The secondary fundamental characteristic is the vibrational spectra of the mineral which depends on the primary fundamental. Such spectra define the molecular as compared to the crystal structure of the mineral. Huminicki and Hawthorne proposed a structural hierarchy for phosphates [6]. This structural

* Corresponding author. Tel.: +61 7 3138 2407; fax: +61 7 3138 1804.
E-mail address: r.frost@qut.edu.au (R.L. Frost).

0022-2860/$ - see front matter © 2013 Elsevier B.V. All rights reserved.
http://dx.doi.org/10.1016/j.molstruc.2013.05.061

hierarchy is an arrangement of crystal structures that reflect systematic changes in the character of the chemical bonds. Hawthorne proposed that structures be classified according to the polymerisation of those cation coordination polyhedra with higher bond valencies. The mineral berlinite ($AlPO_4$) is a framework structure topologically identical to that of quartz with the space group $P3_121$. The mineral augelite [$Al_2(PO_4)(OH)_3$] contains Al in both the octahedral and trigonal-bipyramidal coordinations. The structure in the b-direction linked by chains of phosphate and AlO_5 groups. Augelite has space group $C2/m$ with $Z = 4$. In comparison wavellite [$Al_3(PO_4)_2(OH)_3(H_2O)_4](H_2O)$ is an open framework of corner sharing octahedra and tetrahedra with interstitial water groups held in the interstices by hydrogen bonds.

Interestingly Farmer in his book on the infrared spectra of minerals divided the vibrational spectra of phosphates according to the presence, or absence of water and hydroxyl units in the minerals [7]. In aqueous systems, Raman spectra of phosphate oxyanions show a symmetric stretching mode (ν_1) at 938 cm^{-1}, the antisymmetric stretching mode (ν_3) at 1017 cm^{-1}, the symmetric bending mode (ν_2) at 420 cm^{-1} and the ν_4 mode at 567 cm^{-1} [8–10]. Farmer reported the infrared spectra of berlinite ($AlPO_4$) with PO_4 stretching modes at 1263, 1171, 1130 and 1114 cm^{-1}; bending modes at 511, 480, 451, 379 and 605 cm^{-1}. Al–O modes were found at 750, 705, 698 and 648 cm^{-1}. On hydration of the mineral as with variscite ($AlPO_4{\cdot}2H_2O$), PO_4 stretching modes were found at 1160, 1075, 1050 and 938 cm^{-1}; bending modes at 515, 450 and 420 cm^{-1}; in addition H_2O stretching bands were found at 3588, 3110, 2945 cm^{-1}. For the mineral augelite ($AlPO_4(OH)_3$), infrared bands were observed at 930 (ν_1), 438 (ν_2), 1205, 1155, 1079, 1015 (ν_3) and 615, 556 cm^{-1} (ν_4). For augelite, OH stretching modes were not observed.

Raman spectroscopy has proven most useful for the study of mineral structures [11–16]. The objective of this research is to report the Raman and infrared spectra of senegalite and to relate the spectra to the molecular structure of the minerals. The number of senegalite occurrences is limited [17]. This is the first report of a systematic study of senegalite from Brazil.

2. Experimental

2.1. Mineral

The senegalite sample studied in this work was collected from the Jangada mine, an iron ore deposit located in the Quadrilátero Ferrífero, municipality of Brumadinho, Minas Gerais, Brazil. In the Jangada mine a number of Al and Cu phosphates such as wavellite, turquoise, senegalite, as well as apatite, occur in the weathered zone [18].

In the Jangada mine, yellowish-green crystals of senegalite up to 0.5 mm occur in association with hematite and clay minerals. A complete mineralogical characterization of the Jangada mine was carried out by Nunes [19], including crystallographic study of senegalite. The collected sample was incorporated to the collection of the Geology Department of the Federal University of Ouro Preto, Minas Gerais, Brazil, with sample code SAB-117. The sample was gently crushed and the associated minerals were removed under a stereomicroscope Leica MZ4. Scanning electron microscopy (SEM) was applied to support the chemical characterization and indicate the elements to be analyzed by EMP.

2.2. Scanning electron microscopy (SEM)

Experiments and analyses involving electron microscopy were performed in the Center of Microscopy of the Universidade Federal de Minas Gerais, Belo Horizonte, Minas Gerais, Brazil (http://www.microscopia.ufmg.br).

A senegalite crystal aggregate up to 0.5 mm was coated with a 5 nm layer of evaporated carbon. Secondary Electron and Backscattering Electron images were obtained using a JEOL JSM-6360LV equipment. Qualitative and semi-quantitative chemical analyses in the EDS mode were performed with a ThermoNORAN spectrometer model Quest and was applied to support the mineral characterization.

2.3. Raman spectroscopy

Crystals of senegalite were placed on a polished metal surface on the stage of an Olympus BHSM microscope, which is equipped with 10×, 20×, and 50× objectives. The microscope is part of a Renishaw 1000 Raman microscope system, which also includes a monochromator, a filter system and a CCD detector (1024 pixels). The Raman spectra were excited by a Spectra-Physics model 127 He–Ne laser producing highly polarised light at 633 nm and collected at a nominal resolution of 2 cm^{-1} and a precision of ±1 cm^{-1} in the range between 100 and 4000 cm^{-1}. Repeated acquisition on the crystals using the highest magnification (50×) was accumulated to improve the signal to noise ratio in the spectra. Spectra were calibrated using the 520.5 cm^{-1} line of a silicon wafer.

2.4. Infrared spectroscopy

Infrared spectra were obtained using a Nicolet Nexus 870 FTIR spectrometer with a smart endurance single bounce diamond ATR cell. Spectra over the 4000–525 cm^{-1} range were obtained by the co-addition of 128 scans with a resolution of 4 cm^{-1} and a mirror velocity of 0.6329 cm/s. Spectra were co-added to improve the signal to noise ratio.

Band component analysis was undertaken using the Jandel 'Peakfit' (Erkrath, Germany) software package which enabled the type of fitting function to be selected and allowed specific parameters to be fixed or varied accordingly. Band fitting was done using a Lorentz–Gauss cross-product function with the minimum number of component bands used for the fitting process. The Lorentz–Gauss ratio was maintained at values greater than 0.7 and fitting was undertaken until reproducible results were obtained with squared correlations (r^2) greater than 0.995. Band fitting of the spectra is quite reliable providing there is some band separation or changes in the spectral profile.

3. Results and discussion

3.1. Chemical characterization

The SEM image of senegalite sample studied in this work is shown in Fig. 1. Senegalite crystal aggregates shows tabular to prismatic habitus and orthorhombic form. The mineral occurs in association with hematite and clay minerals not identified. Qualitative chemical analysis shows. The presence of C in the EDS spectra is due to the influence of carbon tape and coating (see Fig. 2).

3.2. Vibrational spectroscopic background

Farmer [7] divided the vibrational spectra of phosphates according to the presence, or absence of water and/or hydroxyl units in the minerals. In aqueous systems, Raman spectra of phosphate oxyanions show a symmetric stretching mode (ν_1) at 938 cm^{-1}, the antisymmetric stretching mode (ν_3) at 1017 cm^{-1}, the symmetric bending mode (ν_2) at 420 cm^{-1} and the ν_4 mode

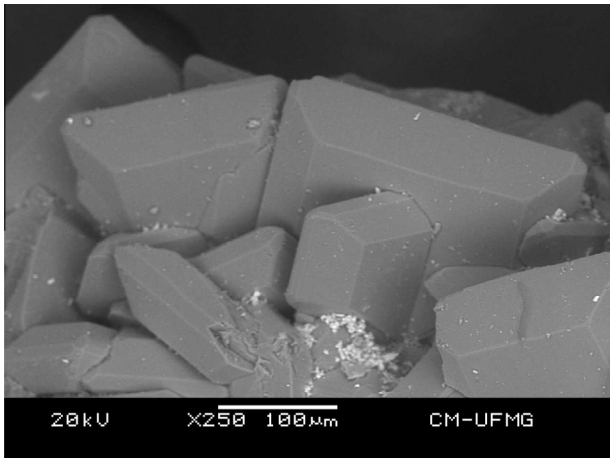

Fig. 1. Backscattered electron image (BSI) of a senegalite fragment up to 0.5 mm in length.

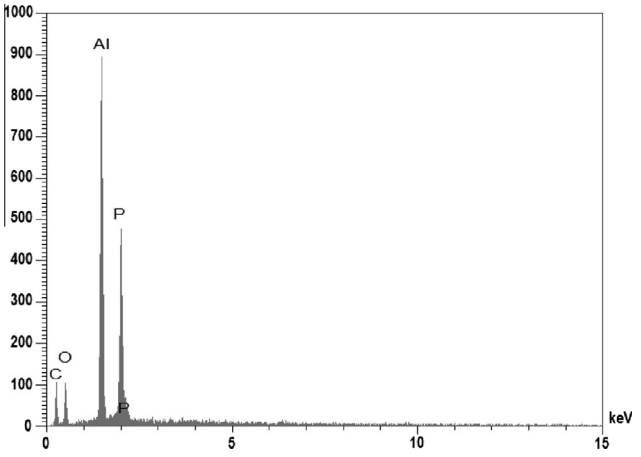

Fig. 2. EDS spectra of senegalite.

at 567 cm^{-1} [8–10,20]. The value for the ν_1 symmetric stretching vibration of PO_4 units as determined by infrared spectroscopy was given as 930 cm^{-1} (augelite), 940 cm^{-1} (wavellite), 970 cm^{-1} (rockbridgeite), 995 cm^{-1} (dufrénite) and 965 cm^{-1} (beraunite). The position of the symmetric stretching vibration is mineral dependent and a function of the cation and crystal structure. The fact that the symmetric stretching mode is observed in the infrared spectrum affirms a reduction in symmetry of the PO_4 units.

The value for the ν_2 symmetric bending vibration of PO_4 units as determined by infrared spectroscopy was given as 438 cm^{-1} (augelite), 452 cm^{-1} (wavellite), 440 and 415 cm^{-1} (rockbridgeite), 455, 435 and 415 cm^{-1} (dufrénite) and 470 and 450 cm^{-1} (beraunite). The observation of multiple bending modes provides an indication of symmetry reduction of the PO_4 units. This symmetry reduction is also observed through the ν_3 antisymmetric stretching vibrations. Augelite shows infrared bands at 1205, 1155, 1079 and 1015 cm^{-1} [21,22]; wavellite at 1145, 1102, 1062 and 1025 cm^{-1}; rockbridgeite at 1145, 1060 and 1030 cm^{-1}; dufrénite at 1135, 1070 and 1032 cm^{-1}; and beraunite at 1150, 1100, 1076 and 1035 cm^{-1}.

3.3. Vibrational spectroscopy

The Raman spectrum of senegalite over the full wavenumber range is displayed in Fig. 3a. This spectrum shows the position of the bands and the relative intensity of these Raman bands. It is noted that there are large parts of the spectrum where little or no intensity is observed. Thus, the spectrum is subdivided into sections based upon the type of vibration being studied. The infrared spectrum over the 500–4000 cm^{-1} spectral range is reported in Fig. 3b. This figure shows the position and relative intensities of the infrared bands of senegalite. As for the Raman spectrum, the infrared spectrum is divided into sections based upon the type of vibration being examined.

The Raman spectrum of senegalite over the 800–1300 cm^{-1} spectral range is reported in Fig. 4a. The Raman spectrum is dominated by an intense sharpish band at 1029 cm^{-1} assigned to the PO_4^{3-} ν_1 symmetric stretching mode. Intense Raman bands are found at 1071 and 1154 cm^{-1} with bands of lesser intensity at 1110, 1179 and 1206 cm^{-1} and are attributed to the PO_4^{3-} ν_3 antisymmetric stretching vibrations. Two other Raman bands are observed at 829 and 892 cm^{-1}. The probable assignation of these bands is to hydroxyl deformation modes.

The infrared spectrum of senegalite over the 800–1300 cm^{-1} spectral range is reported in Fig. 4b. This spectrum shows complexity with a series of overlapping bands. The intense infrared band at 1002 with a shoulder at 1027 cm^{-1} is attributed to the *t* PO_4^{3-} ν_1 symmetric stretching mode. Infrared bands are observed at 1059, 1080, 1101, 1142, 1180, 1193 and 1212 cm^{-1}. These bands are assigned to the PO_4^{3-} ν_1 symmetric stretching vibrations. Two infrared bands are observed at 857 and 899 cm^{-1} and may be attributed to hydroxyl deformation modes.

A comparison may be made with spectra of other aluminium containing phosphate minerals such as augelite [23] and turquoise [24]. In the Raman spectrum of augelite, an intense band is

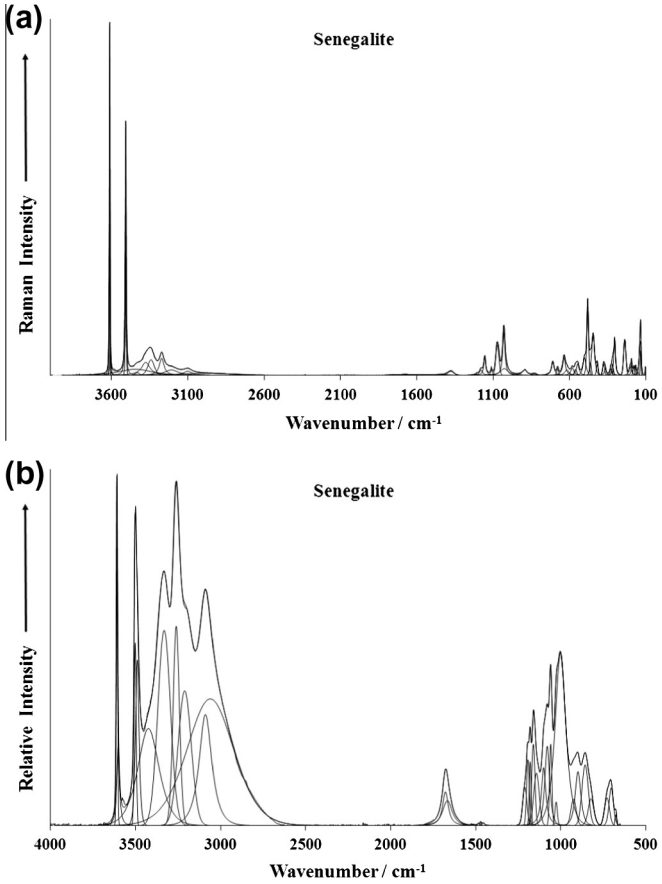

Fig. 3. (a) Raman spectrum of senegalite over the 100–4000 cm^{-1} spectral range. (b) Infrared spectrum of senegalite over the 500–4000 cm^{-1} spectral range.

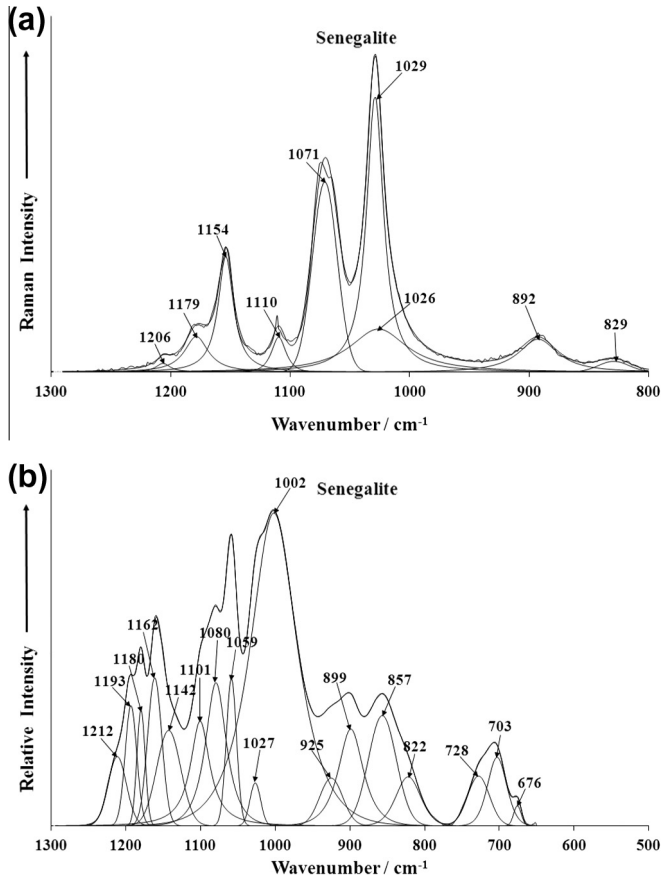

Fig. 4. (a) Raman spectrum of senegalite over the 800–1400 cm^{-1} spectral range. (b) Infrared spectrum of senegalite over the 500–1300 cm^{-1} spectral range.

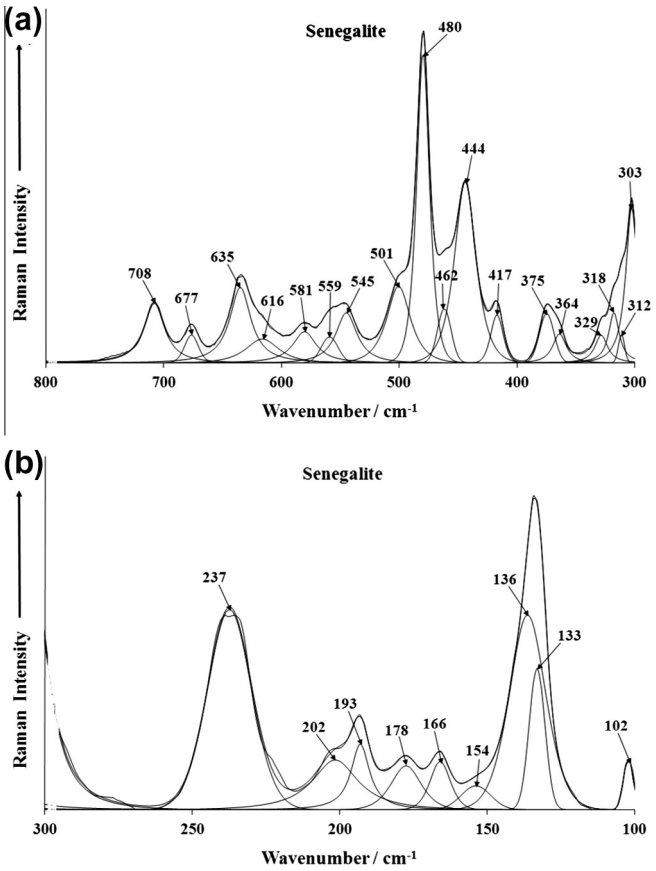

Fig. 5. (a) Raman spectrum of senegalite over the 300–800 cm^{-1} spectral range. (b) Raman spectrum of senegalite over the 100–300 cm^{-1} spectral range.

observed at 1108 cm^{-1}. The band is very sharp with a band width of 7.0. This band is assigned to the ν_1 symmetric stretching mode. Breitinger et al. assigned a band at 1108 cm^{-1} for synthetic augelites to this mode. The position is in sharp contrast to the value of 930 cm^{-1} published by Farmer [7]. In the infrared spectrum the band at 1070 cm^{-1} is assigned to this mode. In the infrared spectrum bands of augelite are observed at 1204, 1171, 1142, 1102, 1070 and 1016 cm^{-1}. The position of these bands may be compared with those reported by Farmer. Bands were given as 1205, 1155, 1079 and 1015 cm^{-1}. The three higher wavenumber bands (1204, 1171, 1142 cm^{-1}) are attributed to the ν_3 antisymmetric PO_4 stretching vibrations. An intense band is observed at 1160 with a resolved component band at 1136 cm^{-1} which may be attributed to these vibrational modes.

For the turquoise from Senegal, Raman bands are observed at 1182, 1161 and 1104 cm^{-1}. Six bands are predicted from group theory, but are not observed and this is attributed to accidental degeneracy. The two sets of Raman bands from the two independent phosphate units overlap. In the infrared spectrum of turquoise, the three higher wavenumber bands at 1195, 1161 and 1109 cm^{-1} are ascribed to the ν_3 antisymmetric stretching vibrations.

The Raman spectra of senegalite in the 300–800 cm^{-1} and in the 100–300 cm^{-1} spectral ranges are displayed in Fig. 5a and b. The first spectrum displays a series of overlapping Raman bands. This spectrum may be subdivided into sections. The first section is the 600–800 cm^{-1} spectral region, the second section is the bands around 500 cm^{-1} and the third section is the bands between 300 and 400 cm^{-1}. Raman bands at 545, 559, 581, 616 and 635 cm^{-1} are assigned to the ν_4 PO_4^{3-} bending modes. The Raman bands at 417, 444, 462, 477 and 480 cm^{-1} are due to the ν_2 PO_4^{3-} bending modes. The two bands at 677 and 708 cm^{-1} may be ascribed to water librational modes. Breitinger et al. [5] reported low intensity bands for synthetic augelite at 750 and 530 cm^{-1} which were assigned to the $\nu(Al(O/OH)_n)$ modes. The Raman spectrum displays a number of bands at 303, 312, 318, 329, 364 and 375 cm^{-1}. It is thought that these bands are due to Al–O stretching vibrations.

In the Raman spectrum of augelite, an intense band is observed at 635 cm^{-1} with component bands at 643 and 615 $cm^{-1}$and are assigned to the ν_4 PO_4 mode. In the infrared spectrum of augelite, the band at 645 cm^{-1} is assigned to this ν_4 PO_4 bending mode. In the Raman spectrum bands are observed at 467, 439, 419 and 407 cm^{-1}. These bands are attributed to the ν_2 bending modes of the PO_4 units. The Raman spectra of turquoise in the 500–700 cm^{-1} spectral range are complex with a significant number of overlapping bands. This spectral region is where the ν_4 phosphate bending modes are expected. For turquoise Raman bands are observed at 643, 593, 570 and 550 cm^{-1}. The results of FGA show that at least two phosphate bending modes would be expected. With loss of degeneracy this number would be expected to increase. For the turquoise from Senegal, Raman bands are observed at 484, 468, 439 and 419 cm^{-1}. For the mineral chalcosiderite two strong bands are observed at 445 and 397 cm^{-1}. These bands are also assigned to the ν_2 bending modes. Raman bands of senegalite in the 100–300 cm^{-1} spectral region are described as lattice vibrations. Intense Raman bands are observed at 136 and 237 cm^{-1}.

Contrasting intensities between the Raman and infrared spectra are found in the 2600–3800 cm^{-1} spectral region (Fig. 6). Intense very sharp Raman bands are observed at 3505 and 3610 cm^{-1} with

shoulders on the high wavenumber side at 3507 and 3614 cm^{-1}. These bands are attributed to OH stretching vibrations. The series of low intensity Raman bands are observed at 3099, 3206, 3270, 3339, 3374 and 3429 cm^{-1} and are assigned to water stretching vibrations. In the infrared spectrum, bands are observed at 3490 and 3609 cm^{-1} with shoulder bands at 3502 and 3603 cm^{-1}. These bands are ascribed to the stretching vibrations of the hydroxyl units. Intense infrared bands are found at 3061, 3089, 3211, 3261, 3332 and 3424 cm^{-1} and are assigned to water stretching vibrations.

There are two crystallographic independent hydrogen bonds in augelite [4] and two of the expected three ν(OH) bands are generated by correlation splitting in the symmetry correlated pairs of the OH groups in general positions. In the infrared spectrum strong bands are observed at 3538, 3453 and 3326 cm^{-1}. Breitinger et al. reported three infrared bands at 3511, 3449 and 3392 cm^{-1} for arseno-augelite [5]. Farmer did not report the OH stretching vibrations of augelite [7]. The two higher wavenumber bands of augelite are assigned to the OH stretching vibrations of the Al_2OH units and the last band to the Al_3OH units. Two intense bands are observed at 3547 and 3468 cm^{-1}.

Two sets of bands for augelite are observed: firstly the bands at 3536, 3524, 3490 and 3479 cm^{-1} and secondly the bands at 3391 and 3376 cm^{-1}. There are two effects being observed. Firstly the separation of the ν(OH) modes in the Al_2OH and Al_3OH groups and secondly the satellite bands caused by the substitution of Al by Fe in these groups. FGA of turquoise predicts two independent water units and four OH units. The vibrational modes are both Raman and infrared active. Thus it is predicted that there should be a four OH symmetric stretching vibrations from the OH units and two from the water units. For the turquoise from Senegal, two intense bands are observed at 3289 and 3093 cm^{-1}. The infrared spectrum of the Senegal turquoise shows greater complexity with infrared bands observed at 3280, 3266, 3076 3069 and 2925 cm^{-1}.

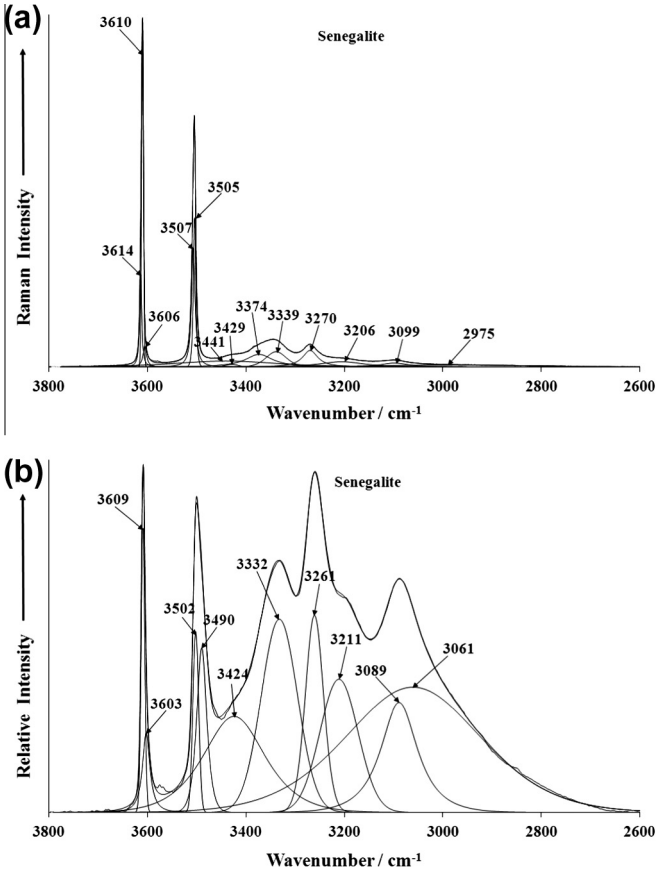

Fig. 6. (a) Raman spectrum of senegalite over the 2600–4000 cm^{-1} spectral range. (b) Infrared spectrum of senegalite over the 2600–4000 cm^{-1} spectral range.

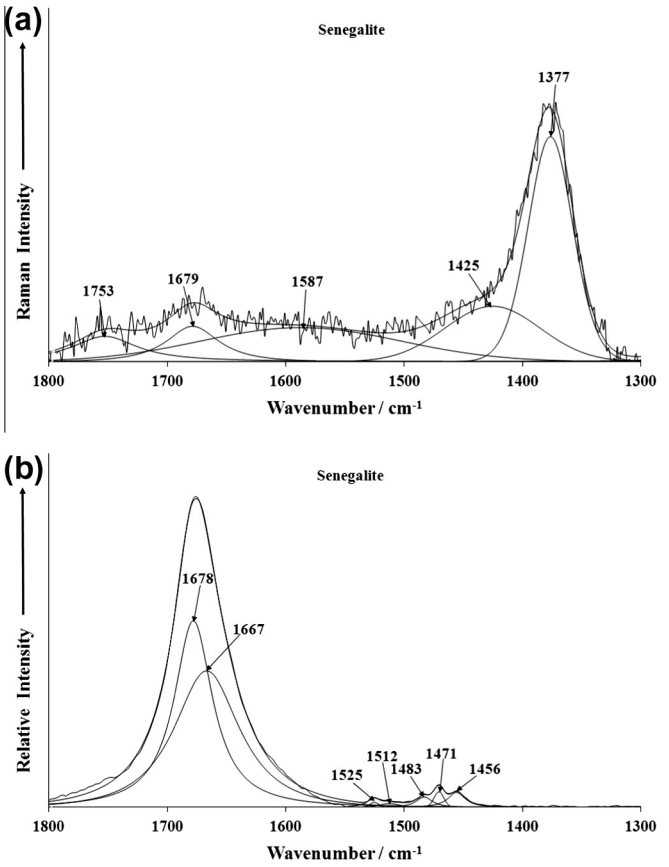

Fig. 7. (a) Raman spectrum of senegalite over the 1300–1800 cm^{-1} spectral range. (b) Infrared spectrum of senegalite over the 1300–1800 cm^{-1} spectral range.

The Raman spectrum of senagalite in the 1300–1800 cm^{-1} spectral range is reported in Fig. 7a. This spectrum suffers from a lack of signal; nevertheless, some Raman bands may be identified. The strongest band is found at 1377 cm^{-1}. The infrared spectrum over this spectral range is illustrated in Fig. 7b. Infrared bands at 1667 and 1678 cm^{-1} are attributed to the water bending modes. The position of these bands indicates strong hydrogen bonding between the water molecules and the phosphate units in the senagalite structure. Low intensity infrared bands are noted at 1456, 1471, 1483, 1512 and 1525 cm^{-1}.

4. Conclusions

We have studied a sample of the phosphate mineral senegalite from the Jangada mine, an iron ore deposit located in the Quadrilátero Ferrífero, municipality of Brumadinho, Minas Gerais, Brazil. The chemical characterization via SEM/EDS shows a homogeneous phase, composed of Al and P. The SEM image of senegalite sample shows crystal aggregates with tabular to prismatic habitus and orthorhombic form.

Senagalite is one of many phosphate minerals containing aluminium and/or ferric iron, including turquoise and augelite. The mineral can be successfully analyzed by Raman spectroscopy and a comparison of the Raman spectrum made with that of turquoise and augelite. The Raman spectrum is dominated by an intense

band at 1029 cm^{-1} assigned to the PO_4^{3-} ν_1 symmetric stretching mode. Raman bands at 545, 559, 581, 616 and 635 cm^{-1} are assigned to the ν_4 PO_4^{3-} bending modes. The Raman bands at 417, 444, 462, 477 and 480 cm^{-1} are due to the ν_2 PO_4^{3-} bending modes. The observation of multiple bending modes offers strong support for the reduction in symmetry of the phosphate anion in the senagalite structure. Intense very sharp Raman bands are observed at 3505 and 3610 cm^{-1} and are attributed to OH stretching vibrations. Vibrational spectroscopy offers a unique means of studying the molecular structure of senagalite.

Acknowledgements

The financial and infra-structure support of the Discipline of Nanotechnology and Molecular Science, Science and Engineering Faculty of the Queensland University of Technology, is gratefully acknowledged. The Australian Research Council (ARC) is thanked for funding the instrumentation. The authors would like to acknowledge the Center of Microscopy at the Universidade Federal de Minas Gerais (http://www.microscopia.ufmg.br) for providing the equipment and technical support for experiments involving electron microscopy. R. Scholz thanks to CNPq – Conselho Nacional de Desenvolvimento Científico e Tecnológico (Grant No. 306287/2012-9).

References

[1] Z. Johan, Lithos 9 (1976) 165–171.
[2] T.D. Keegan, T. Araki, P.B. Moore, Am. Mineral. 64 (1979) 1243–1247.
[3] D. McConnell, Mineral. Mag. 40 (1976) 609–610.
[4] T. Araki, J.J. Finney, T. Zoltai, Am. Mineral. 53 (1968) 1096–1103.
[5] D.K. Breitinger, J. Mohr, D. Colognesi, S.F. Parker, H. Schukow, R.G. Schwab, J. Mol. Struct. 563–564 (2001) 377–382.
[6] D.M.C. Huminicki, F.C. Hawthorne, Rev. Mineral. Geochem. 48 (2002) 123–325.
[7] V.C. Farmer, Mineralogical Society Monograph 4: The Infrared Spectra of Minerals, 1974.
[8] R.L. Frost, W. Martens, P.A. Williams, J.T. Kloprogge, Mineral. Mag. 66 (2002) 1063–1073.
[9] R.L. Frost, W.N. Martens, T. Kloprogge, P.A. Williams, Neues Jahrbuch fuer Mineralogie Monatshefte (2002) 481–496.
[10] R.L. Frost, P.A. Williams, W. Martens, J.T. Kloprogge, P. Leverett, J. Raman Spectrosc. 33 (2002) 260–263.
[11] J. Cejka, J. Sejkora, S. Bahfenne, S.J. Palmer, J. Plasil, R.L. Frost, J. Raman Spectrosc. 42 (2011) 214–218.
[12] R.L. Frost, S. Bahfenne, J. Raman Spectrosc. 42 (2011) 219–223.
[13] R.L. Frost, S. Bahfenne, J. Cejka, J. Sejkora, J. Plasil, S.J. Palmer, E.C. Keeffe, I. Nemec, J. Raman Spectrosc. 42 (2011) 56–61.
[14] R.L. Frost, S.J. Palmer, J. Mol. Struct. 988 (2011) 47–51.
[15] R.L. Frost, S.J. Palmer, H.J. Spratt, W.N. Martens, J. Mol. Struct. 988 (2011) 52–58.
[16] S.J. Palmer, R.L. Frost, J. Raman Spectrosc. 42 (2011) 224–229.
[17] L.H. Coelho, L. Fonseca, K.M. Kaneko, J.C.A. Melo, A origem do fósforo e sua localização espacial nos minérios de ferro enriquecidos supergenicamente, in: II Simp. Bras. Minério de Ferro, ABM, Ouro Preto, 1999, pp. 44–52.
[18] A.P.L. Nunes, M.V. Ribeiro, P.R.G. Brandão, G.E.S. Valadão., Caracterização de Fosfatos Secundários Presentes em Minério de Ferro do Quadrilátero Ferrífero., in: 67 ABM Congress, Rio de Janeiro, 2012.
[19] A.P.L. Nunes, Estudos Eletrocinéticos de Flotabilidade da Wavellita, Turquesa, Senegalita e Apatita, in: Universidade Federal de Minas Gerais, 2012.
[20] R.L. Frost, T. Kloprogge, P.A. Williams, W. Martens, T.E. Johnson, P. Leverett, Spectrochim. Acta Part A Mol. Biomol. Spectrosc. 58A (2002) 2861–2868.
[21] R.L. Frost, Spectrochim. Acta Part A Mol. Biomol. Spectrosc. 60A (2004) 1439–1445.
[22] R.L. Frost, M.L. Weier, K.L. Erickson, O. Carmody, S.J. Mills, J. Raman Spectrosc. 35 (2004) 1047–1055.
[23] R.L. Frost, M.L. Weier, J. Mol. Struct. 697 (2004) 207–211.
[24] R.L. Frost, B.J. Reddy, W.N. Martens, M. Weier, J. Mol. Struct. 788 (2006) 224–231.